Chapter 11
Scaling of the Chewing Muscles in Prosimians

Jonathan M.G. Perry and Christine E. Wall

Contents

11.1 Introduction

The jaw adductor muscles provide the input force for breaking down food. How much force a muscle produces is a function of many variables. Two of the most significant variables are the moment arm (or leverage) of a muscle and its cross-sectional area (Hylander, 1975; Weijs and Hillen, 1985). Muscle forces during mastication have been studied from a theoretical perspective by modeling the mandible as a third-class lever during a static bite (e.g., Hylander, 1975; Greaves, 1978; Smith, 1978; Spencer, 1999). Many studies have compared the leverages of the jaw

---

J.M.G. Perry
Department of Biological Anthropology and Anatomy, Box 3170, Duke University Medical Center, Durham, NC 27710
e-mail: jmp20@duke.edu

C. Vinyard et al. (eds.), *Primate Craniofacial Function and Biology*,
DOI: 10.1007/978-0-387-76585-3_11, © Springer Science+Business Media, LLC 2008

adductor muscles (e.g., Arendsen de Wolff-Exalto, 1951; Smith and Savage, 1959; Smith and Redford, 1990; Vizcaíno et al., 1998), and electromyographic (EMG) data provide a measure of the timing of activity and the relative force of the jaw adductors during mastication (e.g., Hylander and Johnson, 1985; 1994; Hylander et al., 2004; Wall et al., 2006).

Despite a growing data set on muscle leverages and on EMG activity, there are surprisingly few data on cross-sectional area and fiber architecture for the jaw adductor muscles of primates. Such data are critical for integrating theoretical, morphometric, and in vivo work to better understand the muscle forces produced during mastication. Mass has been reported for the chewing muscles of some nonhuman primates (Schumacher, 1961; Cachel, 1979; 1984; Antón, 1999; 2000; Taylor and Vinyard, 2004). Values for cross-sectional area and fiber length have been reported for three species of macaque (Antón, 1999; 2000) and in a comparison of two callitrichid species (Taylor and Vinyard, 2004). Shahnoor et al. (2005) and Anapol et al. (Chapter 9 in this volume) have reported data on the cross-sectional area for 27 primate species. Their data set includes a few prosimians, but prosimians are not the focus of their study.

Here we report the results of a study of the cross-sectional area, mass, fiber length, and pinnation of the jaw adductor muscles of prosimian primates. We measured these variables in 16 prosimian species that span a large range of body sizes and diets (Table 11.1). The goal of this study is to use these data to understand the scaling patterns of the jaw adductor muscles relative to body mass. This is a first step in comparing the force-producing abilities of the jaw adductors across prosimians. In the future, this data set will be expanded to include several other small- and medium-sized prosimians. The complete data set will focus on biomechanical scaling and will also be used to compare feeding adaptations in the jaw muscles and skulls of extant prosimians to Eocene adapids and subfossil lemurs.

As part of the present study, we are comparing the scaling patterns observed in this sample of prosimians to a set of scaling predictions (based on the fracture properties of food) for how the chewing muscles might scale to body mass (Lucas, 2004). The fracture scaling model of Lucas (2004) is an important first attempt to move beyond the assumptions of geometric similarity in predicting the scaling patterns of the chewing muscles relative to body mass (e.g., Cachel, 1979, 1984).

11.1.1 Fiber Architecture

The force a muscle can produce is proportional to its cross-sectional area. A general formula for cross-sectional area is as follows.

$$\text{Area} = \text{muscle mass}/(\text{average fiber length} \times \text{muscle density}) \qquad (11.1)$$

Because much of the mass of a muscle is taken up by sarcomeres in series within a fiber, and because additional length in a muscle fiber does not provide additional force, muscle mass is an inaccurate estimator of muscle force. Even though muscle

Table 11.1 Specimens included in this study

Species	Specimen[a]	Side	Preservation	BM[b](g)	Diet[c]
Avahi laniger laniger	AMNH 170501	L	70% ethanol	1085	mostly leaves
Cheirogaleus medius	DUPC 651m	R		354	fruit and insects
Daubentonia madagascariensis	AMNH 185640	R		742	insect larvae, nuts
Galago senegalensis braccatus	ASU Ef	L	10% formalin	193	mostly insects
	ASU Jf	L			
Galagoides demidoff	NCZP 510f	R		60	mostly insects
	NCZP 507f	L			
Hapalemur griseus	DUPC 1353f	L	Fresh-frozen	940	shoots, stems, leaves
Lemur catta	BAA C2f	L		2207	fruit and leaves
Lepilemur mustelinus leucopus	AMNH 170790m	R	70% ethanol	760	mostly leaves
Mirza coquereli	DUPC 363f	R	Fresh-frozen	320	insects, insect secretions, fruit
Nycticebus coucang	BAA C6m	R		679	mostly insects
Otolemur crassicaudatus	ORPC 1f	L,R	10% formalin	1258	fruits, insects, gum
	ORPC 2f	L,R			
Otolemur garnettii	ASU 1m	L		834	fruits, insects
	Haines Am	L			
Perodicticus potto	AMNH 200640f	R	70% ethanol	1100	fruit and insects
Propithecus verreauxi coquereli	DUPC 6110f	L	Fresh-frozen	3700	leaves, stems, seeds
	DUPC 6560m	R		2780	
Tarsius syrichta	DUPC 89m	R		140	insects and vertebrates
	AMNH 150143f	R	70% ethanol	98	
Varecia variegata rubra	AMNH 201395f	R		3865	mostly fruit

[a] AMNH: American Museum of Natural History Mammalian Collection, ASU: Arizona State University, BAA: Biological Anthropology & Anatomy collection Duke University, DUPC: Duke University Primate Center, Haines: from the collection of Duane Haines, NCZP: North Carolina Zoological Park. All galago specimens courtesy of Dr. N.N. Cordell who dissected the animals. For galagos, the letters following the collection abbreviation are specimen identifiers. The use of 'f' and 'm' designates 'female' and 'male', respectively.

[b] Body Mass. Galago weights are species means for that sex (O.c., O.g., and G.s. from Bearder, 1987; G.d. from Charles-Dominique, 1972). Weights for *Lemur catta* and *Nycticebus coucang* are also species means for that sex (from Sussman, 1991 and Bearder, 1987 respectively). Weights for *Cheirogaleus medius*, *Propithecus verreauxi*, and *Tarsius syrichta* are last-known weights of the individual animals.

[c] Diets for prosimians are generalized and are taken from Nowak, 1999; Sussman, 1999; and Mittermeier et al., 2006.

mass is often the variable reported in publication on muscle anatomy (e.g., Turnbull, 1970; Cachel, 1984), muscle cross-sectional area is the anatomical variable of interest when one wants to estimate muscle forces (e.g., Antón, 1999). However, measuring cross-sectional area is complicated if, as is often the case, fiber architecture is complicated.

Pinnation increases a muscle's ability to generate force by increasing its cross-sectional area compared to that of a parallel-fibered muscle of the same shape and

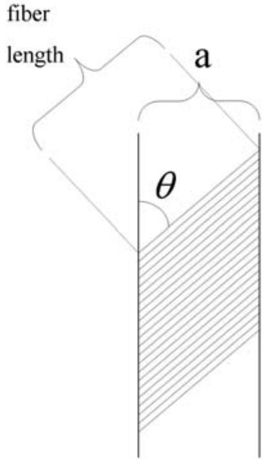

Fig. 11.1 Method of calculating pinnation. Thick vertical lines represent the planes of the surfaces of origin and insertion of the fibers. These surfaces are usually tendinous sheets and are anchored to bone at each end (therefore, the bony attachments of this muscle would be toward the top and bottom of this figure.). Diagonal lines delimit fibers. The angle of pinnation is represented by θ and is calculated as: Sin θ = a/fiber length. Figure modified from Anapol and Barry (1996). Distance "*a*" is the perpendicular distance between tendinous sheets of fiber attachment (mean of at least three measurements at different sites on the muscles). Fiber length was measured after chemical dissolution of connective tissue, and is the mean length of at least 30 measured fibers. We measured fibers from every major region of each muscle

volume (Gans, 1982; Gans and De Vree, 1987). A long, thin muscle in which each fiber originates on a bony surface and inserts on another distant bony surface must have long fibers if it is not pinnate (see Fig. 11.1). However, many muscles are bounded by tendon sheets anchored to (and running perpendicular to) the bony origin and insertion. Generally, in these muscles, many fibers insert on or originate from tendon and the muscle is considered pinnate. In this way, without increasing its volume, the muscle will have more fibers stacked in parallel, and thus it can generate more force.

11.1.2 Scaling Predictions

Previous research suggests that chewing muscle mass in prosimians scales isometrically with body mass (Cachel, 1979, 1984). However, Cachel's sample included only three prosimian species with one specimen each. She concluded that because anthropoids and prosimians together yield a pattern of isometry in chewing muscle mass, and because removal of the prosimians from the regression causes little change in the slope, prosimian chewing muscles scale in the same way as those of anthropoids (isometrically). More data on the prosimians are required to test this conclusion.

Recently, Lucas (2004) generated predictions about how the chewing muscles might scale to body mass. Lucas' "fracture scaling" is a set of predictions about the scaling patterns of the chewing muscles that move beyond assumptions of geometric similarity. Fracture scaling hinges on the fact that particles of food of different sizes fail at different stresses, even if they are homogeneous, equally tough, and deform in a linear-elastic fashion. "Failure" here refers to fragmentation of the particle as cracks propagate through it. Fragmentation is the phenomenon of interest because, in most cases, the purpose of mastication is to break food into smaller pieces.

Lucas compared the fracture properties of two food items of different sizes[1] in a three-point bending model. If the larger item is λ times larger than the smaller one for any linear dimension, it only takes $\lambda^{1.5}$ times as much force to fracture the larger item than the smaller item. Therefore, an 8 cm^3 ($=2^3$) cube of food requires only about 3 ($=2^{1.5}$) times as much force to be fractured as does a 1 cm^3 ($=1^3$) cube of food. If ingested food size is isometric to the size of the animal chewing the food, then this analysis has implications for primate scaling.

Geometric scaling predicts that the chewing muscles should be able to produce λ^2 more force in a larger animal (where the larger animal is λ times larger than the smaller one for any linear dimension). If ingested food size scales isometrically with body size, then a primate that is 8 m^3 in size needs to chew with only about 3 times as much force as a 1 m^3 primate [as opposed to 4 (2^2) times the amount of force – the value predicted by geometry].

Lucas used this relationship, along with the assumption of bite size isometry, to predict that chewing muscle force should scale to the 0.5 power of mass ($M^{0.5}$), and therefore chewing muscle cross-sectional area should scale to the 0.5 power of body mass. This slope is lower than the 0.67 slope predicted by geometric similarity.

From the prediction that fiber length is isometric ($M^{0.33}$) and that PCSA is negatively allometric ($M^{0.5}$), Lucas predicted slight negative allometry for muscle mass ($M^{0.83}$).

11.2 Materials and Methods

One of us (Perry) dissected the masticatory muscles of 16 prosimian species, represented by a total of 22 specimens (see Table 11.1). Some were preserved in 10% formalin, some in 70% ethanol, and others had been frozen since the time of death. Minimal fiber shrinkage is expected in preserved specimens as they were preserved whole with the muscles intact. All specimens had similar degrees of gape after death: most had a small part of the tongue interposed between the incisors (equivalent to 2–5° of gape at the central incisors).

---

[1] Here we are referring to the size of a food item as it is presented to the molars for mastication. This is probably roughly equivalent to the size of a food item as bitten off by the anterior dentition, but very different from the sizes of the food particles that result from the action of mastication.

The chewing muscles of the galago specimens had been examined and removed from the cadavers for previous work (Cordell, 1991). These animals had been preserved with mouth postures similar to those of the other prosimians in this sample. As these muscles were ex situ and muscle orientation could not be determined, it was impossible to accurately measure muscle thickness perpendicular to the line of action. Therefore, no pinnation correction was performed on them (see below).

11.2.1 The Chewing Muscles

Three groups of masticatory adductor muscles were examined: (1) the temporalis group, (2) the masseter group, and (3) the pterygoid group. The pterygoid group includes the medial and lateral pterygoid. The latter is primarily a jaw opener and was not included in this study.

Table 11.2 compares the nomenclature used by various authors to describe the mandibular adductors. The temporalis and masseter group each can be divided into

Table 11.2 Synonyms for masticatory muscle terminology used here

Muscle	Authors in agreement	Synonym
Superficial Masseter (SM)	De Gueldre and De Vree, 1988; Cordell, 1991	masseter pars superficialis (Minkoff, 1968; Schön, 1968), masseter superficialis & masseter intermedius (Gaspard et al., 1973b)
Deep Masseter (DM)	De Gueldre and De Vree, 1988; Cordell, 1991	masseter pars superficialis (Minkoff, 1968; Schön, 1968), superficial part of maxillo-mandibularis (Gaspard et al., 1973b,c)
Zygomatico-mandibularis (ZM)	Fiedler, 1953; De Gueldre and De Vree, 1988; Cordell, 1991	deepest portion of masseter (Starck, 1933), masseter pars profundus (Minkoff, 1968; Schön, 1968), masseter profundus (Gaspard et al., 1973b,c), deep masseter (Taylor and Vinyard, 2004)
Superficial Temporalis (ST)	Minkoff, 1968; De Gueldre and De Vree, 1988; Cordell, 1991	pars temporalis lamina superficialis & pars orbitalis (Gaspard et al., 1973c)
Deep Temporalis (DT)	Minkoff, 1968; Cordell, 1991	pars temporalis lamina profunda (Gaspard et al., 1973c), medial temporalis & deep temporalis (De Gueldre and De Vree, 1988)
Zygomatic Temporalis (ZT)	Fiedler, 1953; Cordell, 1991	zygomatico-mandibularis (Starck, 1933), zygomatico-mandibularis & deep part of maxillo-mandibularis (Gaspard et al., 1973c), suprazygomatic temporalis & posterior zygomaticomandibularis (De Gueldre and De Vree, 1988), zygomatico-mandibularis & maxillo-mandibularis (Ross, 1995)
Medial Pterygoid (MP)	as considered here, there is no disagreement about the medial pterygoid	

individual layers of muscle fibers bounded wholly or partly by layers of connective tissue or bone. The temporalis group consists of the zygomatic temporalis, superficial temporalis, and deep temporalis. The masseter group consists of the superficial masseter, deep masseter, and zygomatico-mandibularis. The medial pterygoid muscle is very complex. Connective tissue sheets divide it into four major compartments of fibers (Gaspard et al. 1973a; pers. obs.). This muscle is impossible to divide into unipinnate layers and was treated differently (see below 'Correcting for Pinnation').

11.2.2 Muscle Mass

Following the removal of a muscle, it was patted gently with a paper towel to remove excess water and wet weight was taken using an electronic scale accurate to 0.001 g. Wet weights were preferred to dry weights for two reasons: first, they better reflect the hydrated condition of muscles in living animals; second, once a muscle is dried, it is impossible to chemically dissect its fibers for information on internal architecture and fiber dimensions (Antón, 1999).

11.2.3 Measuring Fiber Length

To determine the average fiber length for each muscle, we modified a protocol used by Rayne and Crawford (1972) for chemical dissolution of connective tissue. If much connective tissue remains, fibers are very likely to break during extraction and fiber lengths will be greatly underestimated.

To measure fiber length, each muscle was immersed in 10% sulfuric acid and cooked in an oven at 60°C. Cooking time varied between 1 and 6 h based on muscle mass and the amount of connective tissue present. Formalin-preserved, ethanol-preserved, and fresh-frozen muscle fibers were equally easy to extract and measure. However, formalin-preserved muscles took considerably more time to cook.

Muscles have to be monitored carefully as overcooking can cause the muscle to become very fragile and positional relationships within the muscle can be lost. We cooked the muscles in Petrie dishes and, to preserve positional relationships, we recorded the position and orientation of the muscle before placing it in the oven. Muscles were also checked frequently to make sure they were not overcooked.

Once enough connective tissue had been dissolved, the muscle was removed from its dish. Then it was blotted gently between water-soaked paper towels and it was examined under a dissecting microscope equipped with an ocular micrometer (accurate to 0.0825 mm at 25×). We measured 30–60 fibers from each muscle, ensuring that each region of the muscle was represented. Mean fiber length was recorded and used in subsequent equations.

11.2.4 Calculating PCSA

The cross-sectional area of each muscle was calculated from the following formula (Schumacher, 1961):

$$\text{PCSA (cm}^2) = \text{muscle mass (g)}/(\text{fiber length (cm)} \times \text{specific density}) \quad (11.2)$$

PCSA stands for physiological cross-sectional area. The specific density of muscle is taken to be 1.0564 g/cm^3 (Murphy and Beardsley, 1974).

For comparative purposes, the reduced physiological cross-sectional area (RPCSA)[2] of each muscle was calculated from the following formula (Anapol and Barry, 1996):

$$\text{RPCSA (cm}^2) = \text{muscle mass (g)} \times \cos\theta/(\text{fiber length (cm)} \times \text{specific density}) \quad (11.3)$$

The angle of pinnation θ is the angle between the fiber orientation and the line of action of the muscle.[3] RPCSA is used when one wants to measure a single component of the force that a muscle produces (Anapol and Barry, 1996). The effect of using RPCSA instead of PCSA is to remove the component of the muscle mass that produces a force vector that is normal to the line of action. Thus, RPCSA is always smaller than PCSA.

Anapol and Barry (1996) measured fiber length in limb muscles. The limbs in their specimens were in a variety of flexed and extended postures. To correct for inter-individual variability in the length of muscle fibers due to this variable preservation, they measured sarcomere lengths for their muscles and adjusted their average fiber length value based on a standard value for vertebrate sarcomere length (2.5 microns). Because all of our specimens were preserved in a similar mouth posture, we did not adjust the fiber length measurements to reflect a standard vertebrate sarcomere length.

11.2.5 Measuring Pinnation

The angle of pinnation θ was calculated using the following formula (Anapol and Barry, 1996, see also Fig. 11.1):

$$\text{Sin}\,\theta = a/\text{mean fiber length for that unit} \quad (11.4)$$

To calculate θ, it was necessary to obtain mean fiber length for each muscle. Fiber length can be measured directly in a cut section of muscle (Anapol and Barry, 1996; Taylor and Vinyard, 2004), but this can be problematic because it is difficult to know that one is cutting a muscle parallel to its fibers. We had already measured

---

[2] ‘R’ is for ‘reduced’. This follows Anapol and Barry (1996) who use the abbreviation ‘RPCA’ for the same variable.

[3] Here, line of action refers to the direction of pull of a muscle. It can be defined in many different ways. By the method of Anapol and Barry (1996), the line of action is parallel to the tendon sheets of fiber attachment. This may be slightly different from a line drawn from the center of a muscle’s bony origin to the center of its bony insertion.

fiber length in the chemically dissected muscles, so we calculated Equation (11.4) for each muscle using the mean of its measured fiber lengths.

The system of classification of the chewing muscles used here (and described above) is based on the presence of fascial planes. This facilitated the pinnation correction because "a" could be measured as the thickness of a muscle. The average thickness of each unit was measured in the coronal plane, perpendicular to the direction of pull of the muscle (bony origin to bony insertion). This thickness constitutes the perpendicular distance "a" between the surface of *fiber* origin and the surface of *fiber* insertion.

It was impossible to physically separate the thin and twisted sheets of the medial pterygoid muscle for measuring muscle weight and thickness without destroying the muscle. Instead, we measured total medial pterygoid weight and average fiber length for the entire muscle. We then used total medial pterygoid thickness divided by four as "a" in Equation (11.4) to get a value for pinnation. The four layers of medial pterygoid are roughly equal in thickness.

It was not possible to calculate RPCSA for the galagos in this sample. Therefore, the comparison of PCSA to RPCSA excludes the galagos.

11.2.6 Statistical Analysis

Species means for muscle mass, mean fiber length, PCSA, and body mass were derived for each muscle. For each individual prosimian, total PCSA is the sum of the PCSA values for all the muscles. Total adductor mass is the sum of the masses of all the muscles. Total mean fiber length is the grand mean of the mean fiber lengths for the muscles.

In most cases, the last known living weight was used as body mass. However, for the galagos, species mean weights were used because living weights were not known. For most of the American Museum of Natural History specimens, cadaver weights were used because living weights were not known. For the AMNH *Avahi* specimen, species mean weight was used because only the head was preserved.

Chewing muscle variables were regressed against body mass in log space using the reduced major axis (RMA) form of Model II regression. The (S)MATR (Version 1, Falster DS, Warton DI & Wright IJ http://www.bio.mq.edu.au/ecology/SMATR) software package was used to perform the regressions and generate confidence intervals. The F-test in (S)MATR was used to test the observed slopes against the slopes hypothesized by geometric scaling and by fracture scaling.

11.3 Results

Tables 11.3 through 11.6 provide the data for PCSA, RPCSA, muscle mass, and fiber length for the seven mandibular adductor muscles of the 16 prosimian species. Table 11.7 provides the pinnation values for all species as well as the ratio of PCSA to body mass and the ratio of RPCSA to body mass.

Table 11.3 Values of physiological cross-sectional area (PCSA) for sixteen species of prosimians (mm^2)

	Al[a]	Cm	Dm	Gd	Gs	Hg	Lc	Lm
SM[b]	52.02[c]	45.40	70.09	10.73	41.19	147.71	155.81	34.61
DM	77.09	20.05	70.09	2.28	7.99	41.55	49.66	64.75
ZM	49.94	21.25	69.44	2.35	10.74	49.34	35.32	23.39
Masseter Mean	179.05	86.70	209.63	15.36	59.91	238.61	240.79	122.75
ZT	29.10	7.67	80.08	2.50	7.13	44.42	67.38	22.60
ST	53.53	38.14	112.16	6.33	31.65	85.82	84.42	60.90
DT	48.38	37.13	127.68	15.25	58.60	107.41	183.32	50.25
Temporalis Mean	131.01	82.94	319.93	24.08	97.38	237.66	335.12	133.74
MP	90.75	32.63	65.76	6.92	23.12	163.61	118.45	54.70
Sum of Adductors	400.80	202.27	595.31	46.35	180.42	639.88	694.36	311.19
	Mc	Nc	Oc	Og	Pp	Pv	Ts	Vv
SM	46.92	92.89	222.86	209.32	81.50	127.72	45.20	97.61
DM	8.29	64.40	37.11	80.12	48.80	119.40	23.38	94.14
ZM	26.25	40.78	34.10	32.10	32.04	152.81	20.59	126.37
Masseter Mean	81.46	198.07	294.07	321.54	162.34	399.93	89.17	318.13
ZT	with ST[d]	29.73	46.31	26.43	48.64	100.60	9.20	77.13
ST	41.66	90.89	179.82	161.39	54.78	139.07	28.33	111.73
DT	41.62	154.35	244.94	283.73	96.93	211.03	42.05	244.39
Temporalis Mean	83.27	274.97	471.07	471.54	200.35	450.69	79.57	433.25
MP	22.35	88.45	103.74	95.40	70.89	260.07	53.70	117.44
Sum of Adductors	187.08	561.49	868.87	888.49	433.59	1110.69	222.44	868.81

[a] Species name abbreviations are as follows: Al (*Avahi laniger*), Cm (*Cheirogaleus medius*), Dm (*Daubentonia madagascariensis*), Gd (*Galagoides demidoff*), Gs (*Galago senegalensis*), Hg (*Hapalemur griseus*), Lc (*Lemur catta*), Lm (*Lepilemur mustelinus*), Mc (*Mirza coquereli*), Nc (*Nycticebus coucang*), Oc (*Otolemur crassicaudatus*), Og (*Otolemur garnettii*), Pp (*Perodicticus potto*), Pv (*Propithecus verreauxi*), Ts (*Tarsius syrichta*), and Vv (*Varecia variegata rubra*).

[b] Muscle name abbreviations are the same as in Table 11.2.

[c] These values are not corrected for pinnation.

[d] It was not possible to separate the ZT from the ST for *Mirza coquereli*. Therefore, these muscles were analyzed as a single unit for the measurement of PCSA and mass. However, it was possible to isolate fibers of ZT from the ST-ZT muscle mass once the muscle had been cooked. Therefore, an average fiber length value could be obtained for each of ZT and ST.

Tarsius syrichta, *Daubentonia madagascariensis*, and the galagos have high PCSA:body mass ratios (Table 11.7). *D. madagascariensis* specimen has very massive chewing muscles ($\sim$1% of body weight) (see Table 11.5 and Fig. 11.3). However, this specimen was a sub-adult. It had all of its adult dentition, but it weighed 742 g, less than half of the average weight of an adult aye-aye ($\sim$2.5 kg, Sterling et al., 1994). Any conclusions regarding aye-aye muscle scaling are tentative without a fully adult specimen.

Four folivores are included in this study (*Hapalemur griseus*, *Propithecus verreauxi*, *Avahi laniger*, and *Lepilemur mustelinus*). *H. griseus* has relatively large PCSA relative to body mass. *P. verreauxi, A. laniger*, and *L. mustelinus* have low

Table 11.4 Values of reduced physiological cross-sectional area (RPCSA) for twelve species of prosimians (mm^2)

	Al[a]	Cm	Dm	Hg	Lc	Lm	Mc	Nc	Pp	Pv	Ts	Vv
SM[b]	50.47[c]	42.61	69.86	134.09	145.67	33.76	45.18	89.70	80.28	125.03	40.07	97.08
DM	71.56	19.64	69.86	39.47	48.76	60.69	8.11	59.68	48.18	111.57	22.81	91.46
ZM	46.63	20.97	68.61	43.11	34.54	22.42	25.09	38.80	31.64	135.17	18.42	120.07
Masseter Mean	168.67	83.23	208.33	216.67	228.97	116.86	78.38	188.18	160.10	371.78	81.30	308.61
ZT	26.70	7.52	77.83	37.89	62.81	20.89	with ST	28.61	47.05	98.23	9.03	74.87
ST	52.92	37.65	111.52	81.83	83.52	60.40	41.12	86.53	54.22	136.30	27.72	110.75
DT	47.81	36.90	126.05	99.01	180.75	49.78	40.45	141.92	95.41	202.92	40.48	240.09
Temporalis Mean	127.42	82.07	315.41	218.73	327.08	131.06	81.56	257.06	196.68	437.46	77.23	425.72
MP	90.12	32.51	65.69	156.44	118.33	54.23	22.20	88.33	70.57	230.07	53.48	117.03
Sum of Adductors	386.21	197.81	589.43	591.84	674.38	302.15	182.14	533.57	427.35	1039.31	212.01	851.36

[a] Species name abbreviations are the same as in Table 11.3.
[b] Muscle name abbreviations are the same as in Table 11.2.
[c] These values are smaller than the PCSA values because they are corrected to reflect the fraction of muscle mass that contributes to force along the line of action of the muscle (parallel to the tendons of fiber attachment).

values of PCSA and RPCSA relative to body mass[4] (Table 11.7). These folivores have high angles of pinnation relative to other prosimians, so RPCSA is relatively much lower than PCSA (Table 11.7).

Relative to body mass, *Galagoides demidoff* has very long adductor fibers (Table 11.6 and Fig. 11.4). *T. syrichta*, *Galago senegalensis*, and *D. madagascariensis* also have long adductor fibers. Pinnation angles are relatively great in *T. syrichta*, but are relatively small in *D. madagascariensis*. *T. syrichta* has long adductor muscle fibers, but maintains large pinnation angles. *G. demidoff*, *G. senegalensis*, and *T. syrichta* are small-bodied insectivores.

On average, the deep temporalis, followed by the superficial masseter, generally has the greatest cross-sectional area (Tables 11.3 and 11.4). However, the medial pterygoid usually follows; it generally has a large cross-sectional area for its mass. On average, the deep temporalis is the largest part of the adductor muscle mass (Table 11.5). It is followed by the superficial masseter, then the superficial

---

[4] This is not with respect to a particular biological expectation, only relative to the other species in the sample.

Table 11.5 Muscle mass (g) for sixteen species of prosimians

	Al[a]	Cm	Dm	Gd	Gs	Hg	Lc	Lm
SM[b]	0.31[c]	0.20	0.75	0.05	0.25	1.83	1.61	0.20
DM	0.42	0.07	0.75	0.01	0.04	0.44	0.52	0.34
ZM	0.28	0.07	0.99	0.01	0.05	0.29	0.28	0.14
Masseter Mean	1.01	0.34	2.49	0.06	0.34	2.56	2.41	0.68
ZT	0.17	0.05	1.20	0.01	0.05	0.39	0.70	0.19
ST	0.42	0.22	1.65	0.03	0.22	0.87	1.01	0.58
DT	0.41	0.20	2.03	0.06	0.38	0.95	2.18	0.44
Temporalis Mean	1.00	0.47	4.88	0.09	0.64	2.21	3.89	1.21
MP	0.37	0.11	0.60	0.02	0.12	0.85	0.83	0.21
Sum of Adductors	2.38	0.92	7.97	0.18	1.09	5.62	7.13	2.10
	Mc	Nc	Oc	Og	Pp	Pv	Ts	Vv
SM	0.19	0.85	1.58	1.88	1.00	1.67	0.18	1.42
DM	0.03	0.43	0.25	0.71	0.26	1.11	0.09	0.72
ZM	0.08	0.28	0.22	0.12	0.32	1.05	0.07	1.12
Masseter Mean	0.30	1.56	2.04	2.71	1.58	3.83	0.35	3.26
ZT	with ST	0.30	0.39	0.30	0.46	0.89	0.07	1.04
ST	0.22	0.98	1.50	1.35	0.62	1.16	0.19	1.59
DT	0.14	1.59	1.79	1.11	1.25	1.98	0.23	3.62
Temporalis Mean	0.36	2.87	3.67	2.76	2.33	4.03	0.49	6.25
MP	0.09	0.44	0.58	0.52	0.44	1.51	0.19	1.10
Sum of Adductors	0.75	4.87	6.29	5.99	4.35	9.37	1.02	10.61

[a] Species name abbreviations are the same as in Table 11.3.

[b] Muscle name abbreviations are the same as in Table 11.2.

[c] Values are species means.

temporalis. The medial pterygoid has the shortest fibers of all the adductors, on average (Table 11.6). The three parts of the temporalis generally have the longest fibers.

A Mann-Whitney U-test (Zar, 1999) showed that RPCSA values are not significantly lower than PCSA values ($U = 87$, $p > 0.05$.). This result suggests that the fraction of the contractile mass that pulls normal to the line of action is not a statistically significant component of the total muscle cross-sectional area in this sample. However, the total cross-sectional areas for folivores drop considerably when they are corrected for pinnation using RPCSA.

Table 11.8 provides the results of the RMA regression analyses. The 95% confidence intervals for PCSA, muscle mass, and fiber length include isometry for all comparisons, except for the PCSA of the deep masseter and the zygomatic temporalis. The PCSA of each of these muscles is positively allometric relative to body mass and the F-test is significant (DM slope $= 0.953$, $p < 0.023$; ZT slope $= 0.917$, $p < 0.021$). The regression for zygomatico-mandibularis is almost significantly different from isometry and shows positive allometry (slope $= 0.849$, $p < 0.090$).

The observed slopes for most PCSA regressions are significantly higher than the slope of 0.5 predicted by fracture scaling (Lucas, 2004). The one exception is the regression for the superficial masseter (slope $= 0.692$, CI $= 0.479 - 1.001$).

Table 11.6 Fiber length (cm) for sixteen species of prosimians

	Al[a]	Cm	Dm	Gd	Gs	Hg	Lc	Lm
SM[b]	0.56[c]	0.42	1.01	0.41	0.57	1.02	0.97	0.55
DM	0.52	0.33	1.01	0.33	0.49	0.86	1.00	0.50
ZM	0.53	0.31	1.35	0.36	0.42	0.49	0.75	0.57
Masseter Mean	0.54	0.35	1.13	0.37	0.49	0.79	0.91	0.54
ZT	0.55	0.62	1.42	0.42	0.62	0.72	0.98	0.86
ST	0.74	0.55	1.39	0.37	0.65	0.83	1.13	0.90
DT	0.80	0.51	1.51	0.36	0.61	0.72	1.13	0.83
Temporalis Mean	0.70	0.56	1.44	0.38	0.63	0.76	1.08	0.86
MP	0.39	0.32	0.86	0.30	0.48	0.43	0.66	0.36
Sum of Adductors	0.58	0.44	1.22	0.36	0.55	0.72	0.95	0.65
	Mc	Nc	Oc	Og	Pp	Pv	Ts	Vv
SM	0.38	0.87	0.67	0.85	1.16	1.24	0.38	1.38
DM	0.34	0.63	0.63	0.84	0.50	0.88	0.37	0.72
ZM	0.29	0.65	0.61	0.70	0.95	0.65	0.33	0.84
Masseter Mean	0.34	0.72	0.64	0.80	0.87	0.92	0.36	0.98
ZT	0.50	0.96	0.79	1.10	0.90	0.84	0.72	1.28
ST	0.50	1.02	0.79	0.79	1.07	0.79	0.62	1.35
DT	0.32	0.98	0.69	0.74	1.22	0.89	0.52	1.40
Temporalis Mean	0.44	0.98	0.76	0.88	1.06	0.84	0.62	1.34
MP	0.38	0.47	0.53	0.51	0.59	0.55	0.33	0.89
Sum of Adductors	0.39	0.80	0.67	0.79	0.91	0.83	0.47	1.12

[a] Species name abbreviations are the same as in Table 11.3.

[b] Muscle name abbreviations are the same as in Table 11.2.

[c] Values are species means.

Table 11.7 Pinnation values, PCSA values relative to body mass, and RPCSA values relative to body mass

Species	Mean θ[a]	Max θ	DM[b]θ	ZM θ	Sum PCSA/BM	Sum RPCSA/BM
A.l.[c]	14.93	23.44 (ZT)	21.82	20.98	0.343[d]	0.331
C.m.	10.41	20.16 (SM)	11.64	9.23	0.571	0.559
D.m.	7.09	13.61 (ZT)	4.67	8.88	0.694	0.689
G.s.	–	–	–	–	0.935	–
G.d.	–	–	–	–	0.778	–
H.g.	18.66	28.85 (ZT)	12.75	26.22	0.730	0.698
L.c.	12.23	21.22 (ZT)	10.93	12.08	0.315	0.306
L.m.	12.56	20.41 (DM)	20.41	16.58	0.380	0.370
M.c.	12.36	17.14 (ZM)	11.79	17.14	0.585	0.569
N.c.	16.41	23.15 (DT)	22.07	17.92	0.827	0.786
O.c.	–	–	–	–	0.691	–
O.g.	–	–	–	–	1.065	–
P.p.	9.53	14.69 (ZT)	9.13	9.13	0.350	0.346
P.v.	18.29	27.80 (ZM)	20.86	27.80	0.343	0.321
T.s.	15.77	27.56 (SM)	12.70	26.55	1.869	1.782
V.v.	10.70	18.17 (ZM)	13.72	18.17	0.205	0.201

[a] The symbol for the angle of pinnation is θ. Each mean pinnation value is the mean of the pinnation values for the seven adductors for that species (species means).

[b] Muscle name abbreviations are the same as in Table 11.2.

[c] Species name abbreviations are the same as in Table 11.3.

[d] Each PCSA and RPCSA value is the sum of the PCSA or RPCSA values for the seven adductors for that species (species means). PCSA, RPCSA, and body mass values are raw values (not logged).

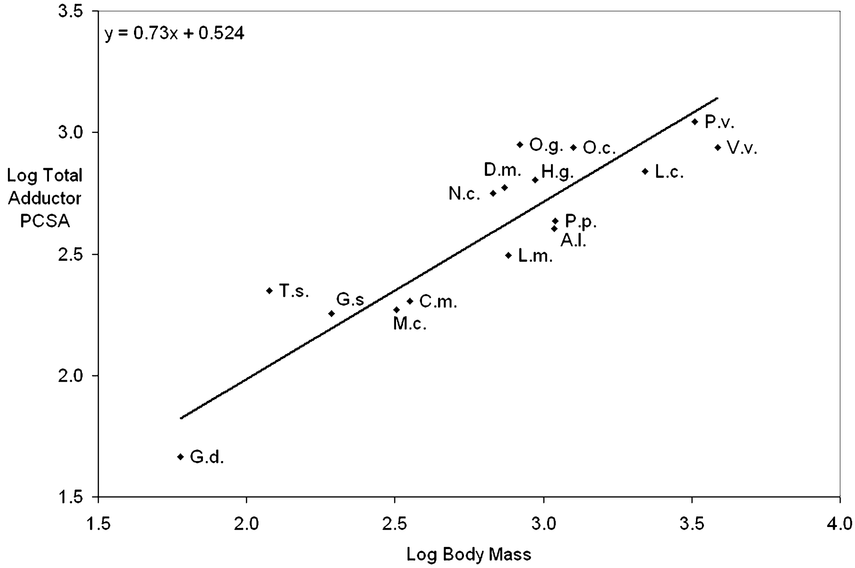

Fig. 11.2 Log of the sum of the PCSA values for all seven adductor muscles plotted against the log of body mass. Values plotted are species means. The line is the reduced major axis fit. Species name abbreviations are the same as in Table 11.3

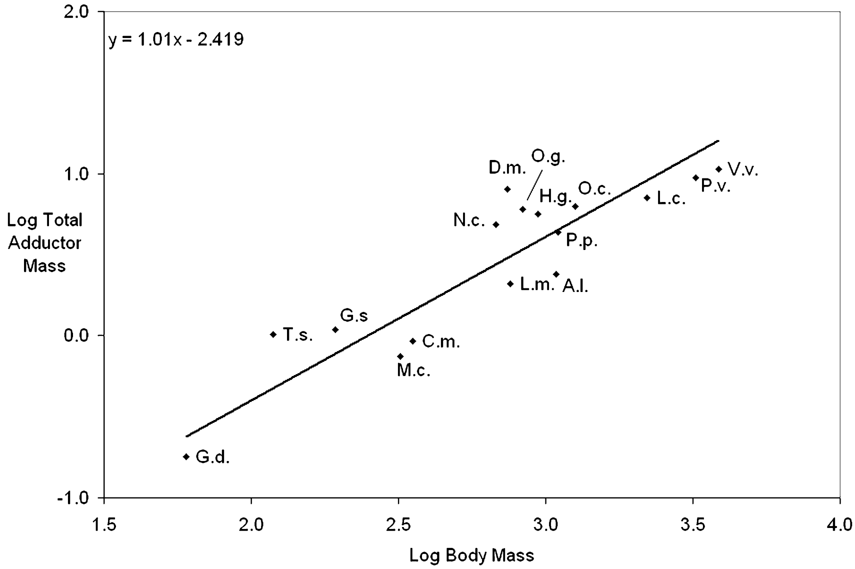

Fig. 11.3 Log of the sum of the muscle mass values for all seven adductor muscles plotted against the log of body mass. Values plotted are species means. The line is the reduced major axis fit. Species name abbreviations are the same as in Table 11.3

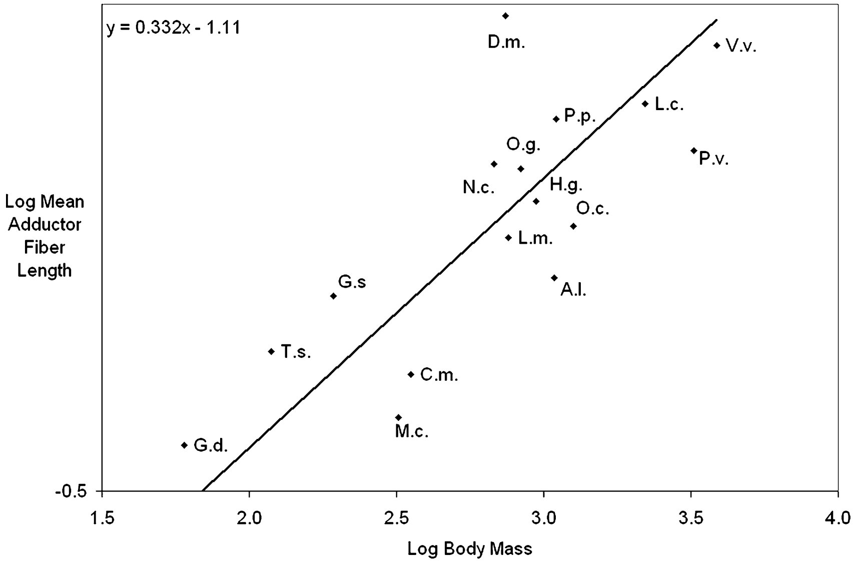

Fig. 11.4 Log of the mean of the fiber length values for all seven adductor muscles plotted against the log of body mass. Values plotted are species means. The line is the reduced major axis fit. Species name abbreviations are the same as in Table 11.3

Table 11.8 Results of reduced major axis (RMA) regressions of muscle dimensions on body mass

Muscle	Slope	R^2	y-intercept	Lower 95% CL	Upper 95% CL	p-value for isometry H_o slope[a]	p-value for fracture scaling H_o slope[b]
Log (10) PCSA vs. Log (10) Body Mass							
DM[c]	0.953	0.72	−1.152	0.707	1.285	0.023*	0.0002**
DT	0.758	0.657	−0.191	0.545	1.053	0.444	0.016*
MP	0.786	0.746	−0.419	0.591	1.045	0.256	0.004**
SM	0.692	0.567	−0.101	0.479	1.001	0.855	0.081
ST	0.737	0.7	−0.292	0.541	1.004	0.524	0.017*
ZM	0.849	0.76	−0.9	0.643	1.12	0.090	0.001**
ZT	0.917	0.788	−1.156	0.706	1.19	0.021*	0.0001**
SUM	0.73	0.777	0.524	0.559	0.954	0.506	0.008**
Log (10) Muscle Mass vs. Log (10) Body Mass							
DM	1.22	0.755	−4.128	0.92	1.62	0.146	0.009**
DT	1.04	0.753	−3.094	0.78	1.37	0.785	0.112
MP	0.974	0.817	−3.244	0.764	1.242	0.819	0.183
SM	1	0.702	−3.102	0.74	1.37	0.982	0.212
ST	0.989	0.748	−3.075	0.745	1.314	0.936	0.210
ZM	1.11	0.781	−3.881	0.85	1.45	0.416	0.033*
ZT	1.13	0.781	−3.845	0.87	1.48	0.333	0.024*
SUM	1.01	0.812	−2.419	0.79	1.3	0.901	0.102

Table 11.8 (continued)

Muscle	Slope	R^2	y-intercept	Lower 95% CL	Upper 95% CL	p-value for isometry H_o slope[a]	p-value for fracture scaling H_o slope[b]
Log (10) Fiber Length vs. Log (10) Body Mass							
DM	0.355	0.543	−1.242	0.243	0.519	0.688	0.688
DT	0.404	0.569	−1.264	0.279	0.583	0.267	0.267
MP	0.296	0.5	−1.158	0.199	0.439	0.572	0.572
SM	0.4	0.659	−1.281	0.288	0.556	0.233	0.233
ST	0.323	0.596	−1.013	0.226	0.462	0.903	0.903
ZM	0.386	0.445	−1.343	0.255	0.584	0.444	0.444
ZT	0.301	0.438	−0.957	0.199	0.458	0.658	0.658
MEAN	0.332	0.628	−1.11	0.235	0.467	0.975	0.975

[a] The slope of isometry is 0.67 for PCSA, 1 for muscle mass, and 0.33 for fiber length.

[b] The slope predicted by fracture scaling is 0.5 for PCSA, 0.83 for muscle mass, and 0.33 for fiber length (Lucas, 2004). An F-test was used to evaluate the significance of the difference between observed slopes and predicted slopes. The p-values reported are for the F-test (as performed in (S)MATR).

[c] Muscle name abbreviations are the same as in Table 11.2.

* Significant difference at the 5% level.

** Significant difference at the 1% level.

The observed slopes for muscle mass relative to body mass are not significantly different from isometry. The observed slopes for some muscle mass regressions (deep masseter, zygomatico-mandibular, and zygomatic temporalis) are significantly different from the slope of 0.83 predicted by fracture scaling. The observed slopes for fiber length are isometric.

Galagoides demidoff, the smallest prosimian in this sample, has a very low total adductor PCSA for its body mass (Fig. 11.2). This datum point has a considerable effect on the regression slope. If it is removed from the total adductor PCSA–body mass regression, the slope drops to 0.648 and is no longer significantly different from either isometry or the fracture scaling slope of 0.5. The addition of other small-bodied prosimians and more *G. demidoff* specimens will help to firm up the slope estimates. *G. demidoff* does have long chewing muscle fibers on average relative to body mass (see Table 11.6 and Fig. 11.4), and this has a necessary negative effect on PCSA for a given muscle mass.

11.4 Discussion

These preliminary results suggest that mandibular adductor PCSA scales with isometry or slight positive allometry relative to body mass in prosimians. Positive allometry of mandibular adductor cross-sectional area is supported by a recent study of a sample that includes both prosimians and anthropoids (Shahnoor et al., 2005; Anapol et al., Chapter 9 in this volume). Lucas (2004:142–144) predicted strong negative allometry of cross-sectional area relative to body mass; the predicted slope is 0.5. No study supports the predicted pattern of strong negative allometry (e.g., $M^{0.5}$) for chewing muscle cross-sectional area (Perry and Wall, 2005; Shahnoor et al., 2005; Anapol et al., Chapter 9 in this volume; this study).

The 95% confidence intervals for the slope of our regressions of PCSA against body mass are very large ($\sim$0.4 for the sum of all adductors, 0.45–0.6 for the individual muscle regressions). Furthermore, the r^2 value is below 0.8 in every case. This suggests that much of the variation in PCSA fails to be explained by variation in body mass.

We plan to examine the biomechanical scaling of cross-sectional area, mass, fiber length, and pinnation of the jaw adductor muscle. Important independent variables to evaluate include the bite force load arms during incisal and molar biting and the moment arms of the jaw muscles (Hylander, 1985).

This sample of prosimians is small and, for most species, only one individual was available. Nevertheless, all families of strepsirrhines were sampled. Five out of nine genera of lorisids (Nowak, 1999; Sussman, 1999) and nine out of fifteen genera of Malagasy lemurs (Mittermeier et al., 2006) were sampled. *Indri*, at the top of the body size range, is very rare, and the only cadaver available was that of a juvenile (studied, but not included here). We will add several more prosimian species to this sample, including many small-sized (e.g., *Microcebus murinus*) and medium-sized (e.g., *Eulemur coronatus*) species. Furthermore, we plan to add an adult aye-aye, another *G. demidoff*, as well as other specimens of *Lemur catta*, *P. verreauxi*, and *Hapalemur griseus*. We expect that the confidence intervals for the regressions will be reduced as a consequence. The gummivores *Elegantulus* and *Phaner*, as well as the greater bamboo lemur *Hapalemur simus*, would make useful additions to this sample. However, cadavers of these species are difficult to obtain.

11.4.1 Cross-Sectional Area, PCSA, RPCSA, and Pinnation

Dietary behavior likely has a strong influence on PCSA. For example, species that chew tough foods may have especially large mandibular adductor PCSA for their body size. Also, species that use large gape may have long chewing muscle fibers and, given isometry in muscle mass, less cross-sectional area relative to body size (cf. Taylor and Vinyard, 2004).

PCSA is low relative to body mass in *Avahi* and *Lepilemur*. It is isometric or nearly so relative to body mass in *Propithecus*. Another way to view this is that the folivores have relatively large body mass compared to their adductor PCSA. Perhaps, this is in part because folivorous prosimians have large gastrointestinal systems that contribute considerable mass to their total body mass (Chivers and Hladik, 1980). Pinnation angles are relatively high in all of these folivores. These data together suggest that folivorous prosimians generate relatively less muscle force for their body mass compared to non-folivorous prosimians of the same size and that a large proportion of this force is normal to the line of action. The moment that the jaw adductors are capable of generating is a function of leverage and force. The short faces and mandibles of *Propithecus*, *Avahi*, and – to a slightly lesser degree – *Lepilemur* and *Hapalemur*, suggest that muscle leverage is high relative to body mass. Estimation of moments generated by the jaw adductors may reveal that greater leverage in the masticatory system of folivorous prosimians (relative to non-folivores) compensates for the small cross-sectional areas of their chewing muscles. Another possibility is that the maximum force required by the mandibular adductors of folivores is smaller than the force required of these muscles in prosimians that exploit other kinds of food. Folivores must chew their food many times, but perhaps each chew demands little muscle force.

The adductor muscles of *Hapalemur griseus* have large PCSA values relative to body mass. This species feeds on bamboo shoots, stems, leaves, fruits, flowers, and fungi in the wild (Overdorff et al., 1997). *Hapalemur* is often considered a folivore for the purposes of studies of functional morphology (e.g., Kay, 1975). However, *Hapalemur* clearly has a different pattern of PCSA compared to *Propithecus*, *Avahi*, and *Lepilemur*.

Slopes were especially high for the PCSA regressions for the deep masseter, zygomatico-mandibularis, and zygomatic temporalis. This suggests that these muscles have especially large cross-sectional areas in the larger prosimians in this sample. If muscle leverage and activity pattern are equal across body sizes in prosimians, these muscles are capable of contributing a larger proportion of the total adductor force in larger prosimians.

The RPCSA of Anapol and Barry (1996) is a necessary modification of PCSA when one is interested in a single component of muscle force (parallel to the line of action), because it reduces muscle mass by the fraction of muscle that generates force *perpendicular* to the line of action. However, incorporating cross-sectional area into models of chewing muscle mechanics is complicated by several factors. First, the chewing muscles have different lines of action. For example, even if all of the fibers of the medial pterygoid were arranged in parallel to its line of action, and the same were true of the deep masseter, these two muscles would still be pulling against one another in the mediolateral plane. Second, many feeding behaviors presumably include mediolateral and anteroposterior muscle forces (e.g., the power stroke of mastication), in addition to vertical force. Pinnate fibers in these muscles might be oblique to the line of action for some masticatory actions, whereas for other actions the same fibers might be parallel to the line of action. Moreover, pinnation angle changes if fibers swivel during concentric or eccentric contractions. Third, chewing muscle force vectors affect food in the occlusal plane. This is a complication because, for example, a vertically oriented muscle vector has a different effect at a vertically oriented occlusal plane than at a horizontally oriented occlusal plane.

Gans (1982) suggested that a muscle layer (or array) should be considered pinnate only if its fibers swivel as they contract. It is unknown if this occurs during jaw adductor contraction in prosimians, though it is likely to occur when fibers originate or insert on connective tissue sheets. Most of the fibers of the medial pterygoid are attached to at least one connective tissue sheet. This is also true of the superficial and deep temporalis, and the superficial and deep masseter. Fewer than half of the fibers in the zygomatico-mandibularis are attached to connective tissue (most attachment is to bone). No fibers of the zygomatic temporalis are attached to a connective tissue sheet, though many converge on a strap-like tendon of insertion.

We are currently working on a modification of the Anapol and Barry (1996) method of correcting for pinnation. This modification will consider different hypothetical lines of action for different masticatory actions. For example, it is possible to correct for pinnation, assuming a vertical line of action for each chewing muscle. For a vertical line of action, pinnation would be measured in the same way as in Equation (11.4), except distance “a” would be measured in the horizontal (i.e., perpendicular to vertical) plane for each muscle, rather than as the distance perpendicular to the tendons of fiber attachment. In choosing the lines of action of interest, reference will be made to the direction of the power stroke of mastication and to the orientation of the occlusal plane.

11.4.2 Fiber Length

Fiber length scales isometrically with body mass in this sample. In this manner, our data conform to the predictions of both geometric and fracture scaling. Deviations from this pattern for individual species may reflect different gape requirements (c.f., Taylor and Vinyard, 2004).

The slopes of regressions of fiber length against body mass have wide confidence intervals and the r^2 values are very low. As with PCSA, much of the variation in fiber length fails to be explained by body mass variation. However, our data do not support the claim that variation in fiber length has *no* relationship to variation in body mass (Antón, 1999; 2000), as all regressions are significant.

It is not surprising that body mass variation explains only some of the variation in fiber length. Fiber length should bear some relation to the range of motion experienced by the lower jaw (Herring and Herring, 1974; Herring et al., 1979). This range of motion is expected to differ based on differences in several factors including jaw and face length, the structural properties of food, the manner of food acquisition, the degree and nature of food processing, and grooming behavior.

It is interesting that the prosimians in this sample, which have the relatively longest fibers, are small-bodied insectivores. *Tarsius* is capable of a large gape (60–70° for *Tarsius bancanus*) and routinely consumes very large animal prey (Jablonski and Crompton, 1994). Immature aye-ayes use gapes of approximately 40° to gnaw holes in wood for extracting insect larvae (Krakauer, 2005).

11.4.3 Muscle Mass

The mass of the mandibular adductors in this sample of prosimians scales isometrically to body mass. Cachel (1979, 1984) found this to be true of primates generally. R-squared values for regressions of muscle mass against body mass range from 0.7 to 0.81. Body mass variation does not explain all of the variation in jaw adductor muscle mass. The 95% confidence intervals for the slope are large for all muscle mass regressions. For all muscles, the confidence interval includes the slope of isometry and, for most, it also includes the slope of 0.83 predicted by fracture scaling. As with PCSA, the muscles that have the highest slopes for regressions of muscle mass against body mass are the deep masseter, zygomatico-mandibularis, and zygomatic temporalis.

Adductor muscle mass is especially great relative to body size for *Daubentonia*, *Tarsius*, and for the larger lorisids. Great adductor mass in these species is likely a result of selection for adductors that produce high forces but that can withstand high degrees of excursion. It is uncertain whether or not adult *Daubentonia* fit this pattern.

11.4.4 Fracture Scaling

Most of the results for scaling of fiber length and muscle mass support the predictions of fracture scaling (Lucas, 2004). However, the predictions regarding cross-sectional area are not supported by the data.

One explanation for the failure of the PCSA data to support the predictions of fracture scaling is that PCSA is an estimator of muscle force (input force), whereas fracture scaling predicts occlusal force (output force), the force needed to fracture foods. The output force differs from the input force because it is modulated by several factors such as muscle activity, muscle leverage, and occlusal morphology. Data on cross-sectional areas of chewing muscles cannot rule out the possibility that *output* muscle force scales with negative allometry relative to body mass.

Another explanation for the lack of correspondence between the observed PCSA scaling patterns and those predicted by fracture scaling is that one or more of the assumptions of fracture scaling is not met by this sample. Lucas (2004) specifically acknowledged that several of these assumptions, such as foods being homogeneous, linearly elastic, and of uniform toughness, are violated in most comparative samples of real primates. Some of these assumptions may be violated in a systematic fashion with respect to body size. For example, larger primates may *generally* feed on tougher foods (e.g., Kay, 1975). It may be difficult to assemble a sample of mammals that vary in body size, but that do not vary with respect to the material properties of the foods they eat.

The fracture scaling model assumes that foods are broken down in three-point bending. This model may be appropriate for many foods, such as nuts and seeds. However, leaves must be cut into many small pieces to be digested efficiently (e.g., Kay and Sheine, 1979). The nutritional contents of some foods, such as juicy fruits and larval insects, may be extracted primarily by tearing or puncturing an outer membrane. Alternately, this may be accomplished by compression/tension. If a different model of food breakdown were used in the fracture scaling equations, different predictions about chewing muscle scaling would result.

The predictions of fracture scaling require that chewing rate scale to the one-quarter power of body mass. However, there is a great deal of variation in the scaling exponents reported for chewing rate (Fortelius, 1985; Druzinsky, 1993). Moreover, chewing rate changes as a bolus of food is reduced (Hiiemae and Kay, 1973), and likely differs with the material properties of food.

Finally, fracture scaling assumes that the size of ingested items scales isometrically with body size. Currently, there are very few data available to evaluate this assumption. While ingested food size may scale isometrically with body mass for some foods, it is likely that there may be little relationship across folivorous primates between body size and the size of ingested leaf materials.

11.5 Conclusions

Based on this sample, the mandibular adductors of prosimians more or less fit the predictions of geometric scaling relative to body mass. Adductor PCSA scales isometrically or with slight positive allometry to body mass. Muscle mass and fiber length scale isometrically to body mass. For most individual adductors and for the sum of all adductors, the PCSA scaling pattern is significantly different from the negative allometry predicted by fracture scaling. The same is true of jaw adductor mass for the deep masseter, the zygomatico-mandibularis, and the zygomatic temporalis. Slopes for jaw adductor mass scaling are not significantly different from the prediction of fracture scaling for any of the other muscles.

Much of the variation in PCSA in prosimians is likely due to differences in food properties and food processing behavior. In this sample, general diet-related patterns of PCSA, muscle mass, and fiber length relative to body mass are not clear. However, the small-bodied folivores, *A. laniger* and *L. mustelinus*, have small PCSA values relative to body mass, whereas *H. griseus* has a high value of PCSA.

The prediction of fracture scaling regarding PCSA was not borne out in this sample. However, we cannot rule out the possibility that activity pattern and muscle leverage modulate input muscle force such that the output occlusal force*does* scale in the manner predicted by Lucas (2004). Regardless, the fracture scaling model has unique merit because its predictions are based on food properties.

As Lucas (2004) pointed out, food properties are likely to affect selection in the masticatory system. Because primate diets are complex, it may be fruitful to modify the fracture scaling model to reflect the complexity of primate chewing rhythms and the many different ways in which primate foods fail during mastication.

Scaling of PCSA to mechanical variables (e.g., load arm length) may yield further insights into adaptation in the jaw adductor muscles (Hylander, 1985). Data on additional prosimian species as well as on the scaling of ingested food size will improve the quality of this ongoing study.

Acknowledgments We thank the Duke University Primate Center (especially S. Combes and J. Ives), the Department of Biological Anthropology & Anatomy (Duke University), the American Museum of Natural History (especially E. Westwig), and Dr. Nancy Cordell for the use of prosimian cadaver material. We thank Drs. R.F. Kay and W.L. Hylander for the use of laboratory space and materials. We thank N.N. Cordell, R.C. Fox, A. Hartstone-Rose, W.L. Hylander, K.R. Johnson, R.F. Kay, A.B. Taylor, C.J. Vinyard, and A.C. Zumwalt for their helpful advice. We thank NSF, NSERC, Duke University, University of Alberta, and Sigma Xi for funding.

References

Anapol, F. and Barry, K. (1996). Fiber architecture of the extensors of the hindlimb in semiterrestrial and arboreal guenons. *Am. J. Phys. Anthropol.* 99:429–447.

Antón, S. C. (1999). Macaque masseter muscle: internal architecture, fiber length, and cross-sectional area. *Int. J. Primatol.* 20:441–462.

Antón, S. C. (2000). Macaque pterygoid muscle: internal architecture, fiber length, and cross-sectional area. *Int. J. Primatol.* 21:131–156.

Arendsen de Wolff-Exalto, E. (1951). On differences in the lower jaw of animalivorous and herbivorous mammals I and II. *Proc. K. Ned. Akad. Wet. C* 54:237–246, 405–410.

Bearder, S. K. (1987). Lorises, bushbabies, and tarsiers: diverse societies in solitary foragers. In: Smuts, B. B., Cheney, D. L., Seyfarth, R. M., Wrangham, R. W. and Struhsaker, T. T. (eds.), *Primate Societies*, The University of Chicago Press, Chicago, pp. 11–24.

Cachel, S. M. (1979). A functional analysis of the primate masticatory system and the origin of the anthropoid post-orbital septum. *Am. J. Phys. Anthropol.* 50:1–18.

Cachel, S. M. (1984). Growth and allometry in primate masticatory muscles. *Arch.Oral Biol.* 29:287–293.

Charles-Dominique, P. (1972). Écologie et vie sociale de *Galago demidovii* (Fisher 1808; Prosimii). *Z. Tierpsychol., Beiheft* 9:7–41.

Chivers, D. J. and Hladik, C. M. (1980). Morphology of the gastrointestinal tract in primates: comparisons with other mammals in relation to diet. *J. Morphol.* 166:337–386.

Cordell, N. N. (1991). *Craniofacial Anatomy and Dietary Specialization in the Galagidae*. Ph.D. Dissertation, University of Washington, Seattle.

De Gueldre, G. and De Vree, F. (1988). Quantitative electromyography of the masticatory muscles of *Pteropus giganteus* (Megachiroptera). *J. Morphol.* 196:73–106.

Druzinsky, R. E. (1993). The time allometry of mammalian chewing movements: chewing frequency scales with body mass in mammals. *J. Theor. Biol.* 160:427–440.

Falster, D. S., Warton, D. I., and Wright I. J., (S)MATR: standardised major axis tests and routines, Version 1.0, 2003, Sydney (August 15, 2006); http://www.bio.mq.edu.au/ecology/SMATR

Fortelius, M. (1985). Ungulate cheek teeth: developmental, functional and evolutionary interrelationships. *Acta Zool. Fennica* 180:1–76.

Gans, C. (1982). Fiber architecture and muscle function. *Exerc. Sport Sci. Rev.* 10:160–207.

Gans, C. and De Vree, F. (1987). Functional bases of fiber length and angulation in muscle. *J. Morphol.* 192:63–85.

Gaspard, M., Laison, F. and Mailland, M. (1973a). Organisation architecturale et texture des muscles ptérygoïdiens chez les primates supérieurs. *J. Biol. Buccale* 1:215–233.

Gaspard, M., Laison, F. and Mailland, M. (1973b). Organisation architecturale et texture du muscle masseter chez les primates et l'homme. *J. Biol. Buccale* 1:7–20.

Gaspard, M., Laison, F. and Mailland, M. (1973c). Organisation architecturale du muscle temporal et des faisceaux de transition du complexe temporo-massétérin chez les primates et l'homme. *J. Biol. Buccale* 1:171–196.

Greaves, W. S. (1978). The jaw lever system in ungulates: a new model. *J. Zool. (Lond.)* 184:271–285.

Herring, S. W., Grimm, A. F., and Grimm, B. R. (1979). Functional heterogeneity in a multipinnate muscle. *Am. J. Anat.* 154:563–576.

Herring, S. W. and Herring, S. E. (1974). The superficial masseter and gape in mammals. *Am. Nat.* 108:561–576.

Hiiemae, K. M. and Kay, R. F. (1973). Evolutionary trends in the dynamics of primate mastication. In: Zingeser, M. R. (ed.), *Symposia of the Fourth International Congress of Primatology, Volume 3: Craniofacial Biology of Primates*. Karger, Basel, pp. 28–64.

Hylander, W. L. (1975). The human mandible: lever or link? *Am. J. Phys. Anthropol.* 43:227–242.

Hylander, W. L. (1985). Mandibular function and biomechanical stress and scaling. *Am. Zool.* 25:315–330.

Hylander, W. L. and Johnson, K. R. (1985). Temporalis and masseter muscle function during incision in macaques and humans. *Int. J. Primatol.* 6:289–322.

Hylander, W. L. and Johnson, K. R. (1994). Jaw muscle function and wishboning of the mandible during mastication in macaques and baboons. *Am. J. Phys. Anthropol.* 94:523–547.

Hylander, W. L., Vinyard, C. J., Ravosa, M. J., Ross, C. F., Wall, C. E., and Johnson, K. R. (2004). Jaw adductor force and symphyseal fusion. In: Anapol, F., German, R. Z. and Jablonski, N. G. (eds.), *Shaping Primate Evolution*. Cambridge University Press, Cambridge, pp. 229–257.

Jablonski, N. G. and Crompton, R. H. (1994). Feeding behavior, mastication, and tooth wear in the Western Tarsier (*Tarsius bancanus*). *Int. J. Primatol.* 15:29–59.

Kay, R. F. (1975). The functional adaptations of primate molar teeth. *Am. J. Phys. Anthropol.* 43:195–216.

Kay, R. F. and Sheine, W. S. (1979). On the relationship between chitin particle size and digestibility in the primate *Galago senegalensis*. *Am. J. Phys. Anthropol.* 50:301–308.

Krakauer, E. B. (2005). *Development of Aye-aye (*Daubentonia madagascariensis*) Foraging Skills: Independent Exploration and Social Learning*. Ph.D. Dissertation, Duke University, Durham.

Lucas, P. W. (2004). *Dental Functional Morphology: How Teeth Work*. Cambridge University Press, Cambridge.

Minkoff, E. C. (1968). *A Study of the Head, Neck, and Forelimb Muscles in the Genus* Galago*(Primates, Lorisidae).* Ph.D. Dissertation, Harvard University, Cambridge.

Mittermeier, R. A., Konstant, W. R., Hawkins, F., Louis, E. E., Langrand, O., Ratsimbazafy, J., Rasoloarison, R., Ganzhorn, J. U., Rajaobelina, S., Tattersall, I. and Meyers, D. M. (2006). *Lemurs of Madagascar*, 2nd ed. Conservation International, Washington, D.C.

Murphy, R. A. and Beardsley, A. C. (1974). Mechanical properties of the cat soleus muscle *in situ*. *Am. J. Physiol.* 227:1008–1013.

Nowak, R. M. (1999). *Walker's Primates of the World*. The Johns Hopkins University Press, Baltimore.

Overdorff, D. J., Strait, S. G., and Telo, A. (1997). Seasonal variation in activity and diet in a small-bodied folivorous primate, *Hapalemur griseus*, in southeastern Madagascar. *Am. J. Primatol.* 43:211–223.

Perry, J. M. G. and Wall, C. E. (2005). A study of the scaling patterns of physiological cross-sectional area of the chewing muscles in prosimians. *Am. J. Phys. Anthropol.* 40S:165.

Rayne, J. and Crawford, G. N. C. (1972). The relationship between fibre length, muscle excursion and jaw movement in the rat. *Arch. Oral Biol.* 17:859–872.

Ross, C. F. (1995). Muscular and osseous anatomy of the primate anterior temporal fossa and the functions of the postorbital septum. *Am. J. Phys. Anthropol.* 98:275–306.

Schön, M. A. (1968). The muscular system of the Red Howling Monkey. *U. S. Nat. Mus. Bull.* 273:1–185.

Schumacher, G. H. (1961). *Funktionelle Morphologie der Kaumuskulatur*. Fisher, Jena.

Shahnoor, N., Anapol, F., Ross, C. (2005). Scaling of reduced physiological cross-sectional area in primate masticatory muscles. *Am. J. Phys. Anthropol.* 40S:188.

Smith, J. M. and Savage, R. J. G. (1959). The mechanics of mammalian jaws. *Sch. Sci. Rev.* 141:289–301.

Smith, K. K. and Redford, K. H. (1990). The anatomy and function of the feeding apparatus in two armadillos (Dasypoda): anatomy is not destiny. *J. Zool.* (London) 222:27–47.

Smith, R. J. (1978). Mandibular biomechanics and temporomandibular joint function in primates. *Am. J. Phys. Anthropol.* 49:341–350.

Spencer, M. A. (1999). Constraints on masticatory system evolution in anthropoid primates. *Am. J. Phys. Anthropol.* 108:483–506.

Starck, D. (1933). Die Kaumuskulatur der Platyrrhinen. *Gegenbaurs Morphologisches Jahrbuch* 72:212–285.

Sterling, E. J., Dierenfeld, E. S., Ashbourne, C. J. and Feistner, A. T. C. (1994). Dietary intake, food composition and nutrient intake in wild and captive populations of *Daubentonia madagascariensis*. *Folia Primatol.* 62:115–124.

Sussman, R. W. (1991). Demography and social organization of free-ranging *Lemur catta* in the Beza Mahafaly Reserve, Madagascar. *Am. J. Phys. Anthropol.* 84:43–58.

Sussman, R. W. (1999). *Primate Ecology and Social Structure: Volume 1: Lorises, Lemurs and Tarsiers*. Pearson Custom Publishing, Needham Heights, MA.

Taylor, A. B. and Vinyard, C. J. (2004). Comparative analysis of masseter fiber architecture in tree-gouging (*Callithrix jacchus*) and nongouging (*Saguinus oedipus*) callitrichids. *J. Morphol.* 261:276–285.

Turnbull, W. D. (1970). Mammalian masticatory apparatus. *Fieldiana: Geol.* 18:147–356.

Vizcaíno, S. F., De Iuliis, G. and Bargo, M. S. (1998). Skull shape, masticatory apparatus, and diet of *Vassallia* and *Holmesina* (Mammalia: Xenarthra: Pampatheriidae): when anatomy constrains destiny. *J. Mammal. Evol.* 5:291–322.

Wall, C. E., Vinyard, C. J., Johnson, K. R., Williams, S. H., and Hylander, W. L. (2006). Phase II jaw movements and masseter muscle activity during chewing in *Papio anubis. Am. J. Phys. Anthropol.* 129:215–224.

Weijs, W. A. and Hillen, B. (1985). Physiological cross-section of the human jaw muscles. *Acta Anat.* 121:31–35.

Zar. J. H. (1999). *Biostatistical Analysis*, 4th ed. Pearson Education (Singapore) Pte. Ltd., Delhi, India.